INT. J. ELECTRONICS, 1975, VOL. 38, NO. 4, 485–512

Measurement of loop gain in feedback systems†

R. D. MIDDLEBROOK‡

In the design of a feedback system it is desirable to make experimental measurements of the loop gain as a function of frequency to ensure that the physical system operates as analytically predicted or, if not, to supply information upon which a design correction can be based. In high loop-gain systems it is desirable that the loop-gain measurement be made without opening the loop. This paper discusses practical methods of measuring and interpreting the results for loop gain of the closed-loop system by a voltage injection or a current-injection technique; extension to the case in which the measurement can be made even though the system is unstable; and extension to the case in which neither the voltage nor current-injection technique alone is adequate, but in which a combination of both permits the true loop gain to be derived. These techniques have been found useful not only in linear feedback systems but also in describing-function analysis of switching-mode converters and regulators.

1. Introduction

In approaching a system design problem, the usual procedure is to make a preliminary paper design and analysis, then to build a breadboard and make experimental tests of the performance. If discrepancies are found between the predicted and observed properties of the system, the analysis model is corrected in a manner suggested by the nature of the observed discrepancies, and the modified predicted performance again compared with the experimental results. Several iterations of the analysis—measurement—correction sequence may be required before final adoption of the system design.

When the system being designed incorporates a negative feedback loop, one of the important performance parameters to be predicted analytically and experimentally verified is the loop gain. This paper is concerned with experimental methods of making such measurements with emphasis on practical problems of accuracy and proper interpretation of the results. These techniques have been found useful not only in linear feedback systems, but also in the describing-function analysis of many types of switching-mode converters and regulators.

The method of measuring loop gain T by injection of either a test voltage or a test current into the loop is first reviewed. The important feature of this method is that the loop remains closed, so that operating points are not disturbed. Use of a narrow-band voltmeter permits loop-gain measurements to be made in high-gain systems, and also in systems in which there is a large amount of noise as, for example, in a switching-mode regulator. A technique for determination of phase as well as magnitude of the loop gain, with use of

Received 23 September 1974.

† This work is an extension of material presented at the ESTEC Spacecraft Power Conditioning Electronics Seminar, ESRIN Centre, Frascati, Italy, 20–22 May 1974.

‡ Professor of Electrical Engineering, California Institute of Technology, Pasadena, California.

magnitude measurements only, is discussed and elimination of possible ill-conditioning of the phase formula by means of suitably scaled magnitude measurements is presented.

Several extensions of this basic method of loop-gain measurement are introduced, and it is first shown how an unstable loop gain can be measured directly. An example is given in which the phase margin is measured to be $-6°$.

For the voltage injection form of the loop-gain measurement method to give the correct result, it is necessary that the injection be performed at a point in the loop at which the impedance Z_2 looking 'backward' from the injection point is sufficiently smaller than the impedance Z_1 looking 'forward' from the injection point. The opposite condition, $Z_2 \gg Z_1$, is necessary for the current injection technique to give a correct result. Since in a practical system it may not be possible to find an injection point that satisfies either of these extreme conditions, at least over the entire frequency range of interest, it is desirable to extend the loop-gain-measurement method to be applicable at an injection point where the impedance ratio Z_2/Z_1 is arbitrary.

It is shown that the true loop gain T can be derived from measurements of ratios T_v and T_i obtained respectively by successive voltage and current injection at a point of arbitrary impedance ratio. The method is illustrated by a practical example, which is also used to demonstrate an inherent accuracy defect in the method, namely, that poor accuracy in the derived T is obtained at frequencies beyond loop-gain crossover when $|T| < 1$.

The inherent accuracy defect is eliminated in an improved method of loop-gain measurement by simultaneous voltage and current injection at a point of arbitrary impedance ratio. In this 'null double-injection' method, the true loop gain T is derived from measurements of ratios T_v^n and T_i^n obtained by adjustment of the relative magnitude and phase of the injected voltage and current to null out the current looking backward from the double-injection point, for T_v^n, and the voltage looking backward, for T_i^n. The null double-injection method is illustrated by an example in which accurate results are obtained for a loop gain T that has an additional pole beyond the cross-over frequency, an example which is particularly poorly conditioned for application of the successive voltage and current-injection method.

Finally, reconsideration is given to the method of loop-gain measurement by simple voltage or current injection alone, and the conditions to be satisfied by the impedance ratio Z_2/Z_1 at the signal injection point are discussed in further detail.

2. Measurement of loop gain in a closed loop by voltage injection or by current injection

In principle, loop gain T can be measured by opening a feedback loop at an appropriate point, application of a test signal in the 'forward' direction at the opened point, and measurement of the resulting loop-transmitted signal that appears looking 'backward' at the opened point.

More specifically, one such 'appropriate point' is at the output of a dependent voltage generator within the feedback loop, as indicated in Fig. 1 (a). The closed loop is defined by a proportionality between the voltage developed by the dependent voltage generator and a signal (either voltage or current) at the impedance Z. (Notation: independent generators are represented by circles, dependent generators by squares.) If the loop is opened and a test voltage v_x applied at point A_v, and the resulting voltage v_y of the dependent generator measured, then, by definition, the loop gain is given by $T=v_y/v_x$. Since the loop is open, a voltage $v_z=v_x+v_y$ appears across the break, as shown in Fig. 1 (a).

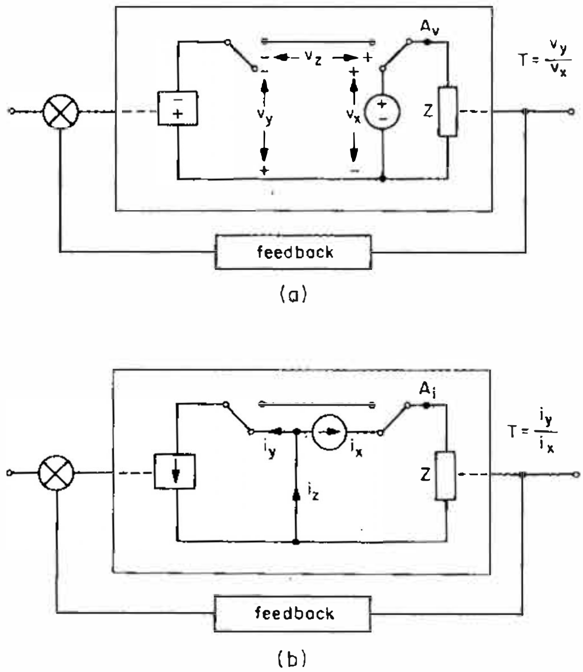

Figure 1. Measurement of loop gain T by opening the loop, (a) by voltage ratio, (b) by current ratio.

Another 'appropriate point' is at the output of a dependent current generator, as indicated in Fig. 1 (b). In this case, 'opening the loop' implies short-circuiting the output of the dependent current generator, and the loop gain, by definition, is $T=i_y/i_x$, where i_y is the dependent generator current resulting from the test current i_x applied at point A_i. Since the loop is open, a current $i_z=i_x+i_y$ flows in the common connection as shown in Fig. 1 (b).

In many practical situations it is inconvenient to open the feedback loop in order to make such loop-gain measurements because, particularly in high-gain systems, it is difficult to maintain proper d.c. operating conditions, and the system may saturate on noise. However, the voltage conditions of Fig. 1 (a) can be maintained without opening the loop by the simple expedient of making v_z, instead of v_x, the independent test signal: as shown in Fig. 2 (a), the original closed-loop circuit topology is retained, and although v_x and v_y are now both dependent quantities, the loop gain is still $T=v_y/v_x$. Similarly, in the dual method shown in Fig. 2 (b), substitution of i_z as the independent test signal permits the original circuit topology to be retained and the loop gain is still $T = i_y/i_x$. Thus, in either method, *injection* of a test signal enables a direct measurement of loop gain to be made without opening the loop.

In a convenient practical implementation of the current-injection method, a test oscillator voltage output is converted to the current i_z by a high resistance and is injected via a blocking capacitor, and the resulting currents i_x

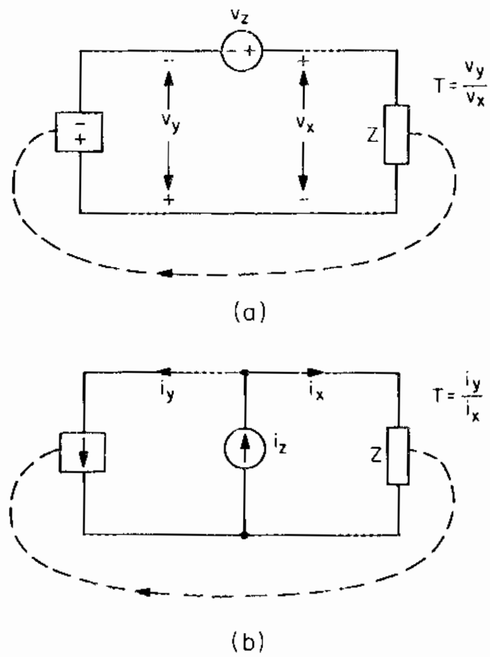

Figure 2. Measurement of T by injection into the closed loop, (a) by voltage ratio, (b) by current ratio.

and i_y are measured by a clip-on current probe attached to a current-to-voltage converter amplifier connected to a voltmeter input. For the voltage-injection method, a clip-on current probe is connected to the oscillator output and used 'backwards' as a one-turn secondary transformer to inject the voltage v_z, and the resulting voltages v_x and v_y are read directly by the voltmeter. Although other methods are possible (*Electron. Design*, 1965), the use of the current probe as a signal-injection transformer is a very convenient way of obtaining the necessary 'floating' voltage v_z. In the voltage-injection method, larger injection voltages can be obtained by wrapping the lead more than once around the clip-on probe, thus increasing the number of 'secondary' turns.

Since the voltage-injection and current-injection methods are duals of each other, it is convenient to refer to the three signals as u_x, u_y and u_z, where u is to be interpreted as either v or i as appropriate. Thus, for either method,

$$u_z = u_x + u_y \tag{1}$$

$$T = \frac{u_y}{u_x} \tag{2}$$

The signals u_x, u_y and u_z are phasors, and so use of an ordinary voltmeter gives directly only the magnitude $|T|$ of the loop gain. Often, it is known that the system being measured is minimum-phase, and so a measurement of loop-gain magnitude is sufficient. However, if phase measurements are desired, a phase-reading voltmeter such as the Princeton Applied Research Two-Phase/Vector Lock-In Amplifier Model 129 may be used. This instrument has the additional advantage that it is phase-locked to the test oscillator signal, and so functions as a narrow-band tracking voltmeter capable of reading very small signals that would otherwise be buried in noise. Indeed, the narrow-band property may be essential in order to make even the magnitude measurements, because in a system with high loop gain, $u_y \gg u_x$ and the allowable magnitude of u_y is limited by system overloading; consequently, u_x is very small and may only be extracted from noise by use of a narrow-band voltmeter. Also, the narrow-band property is especially advantageous in making loop-gain measurements on switching regulators, since otherwise the switching noise would be likely to swamp out at least the smaller of the loop-gain test signals.

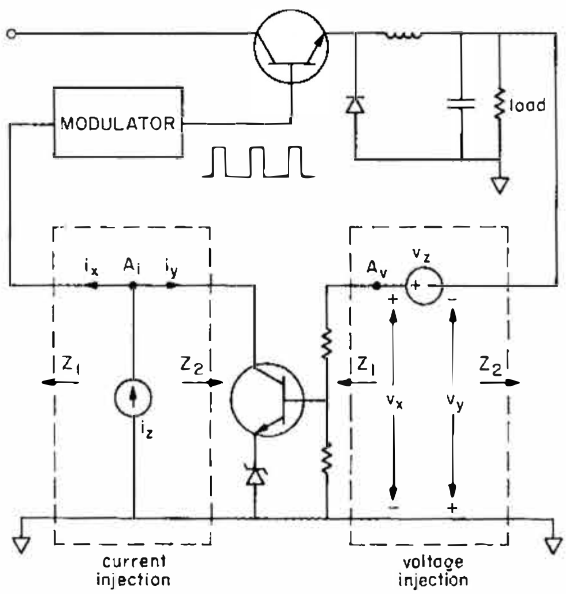

Figure 3. Appropriate points for voltage and for current injection to measure loop gain of a simple switching regulator.

An example of the application of the signal-injection technique for measurement of the loop gain of a simple switching regulator is shown in Fig. 3. As indicated, suitable injection points A_v and A_i for voltage and current injection respectively can be found. The location A_v is suitable for voltage injection because the impedance Z_1 looking forward around the loop is much greater than the impedance Z_2 looking backward, so that v_y approximates the voltage of an ideal voltage generator, as required for the model of Fig. 2 (a) to be valid. Conversely, the location A_i is suitable for current injection because here the opposite condition $Z_2 \gg Z_1$ obtains, so that i_y approximates the current of an ideal current generator (namely, the collector of a transistor), as required for the model of Fig. 2 (*b*) to be valid.

Although it provides directly only magnitude information, a wave analyser such as one of the Hewlett–Packard 302A series is a very convenient instrument for use in the signal-injection method of loop-gain measurement (Spohn 1963, *Hewlett-Packard Application Note*, 1965).† In the 'BFO' mode the instrument operates as an adjustable-frequency oscillator with an automatically tracking narrow-band voltmeter, and thus provides both the test signal and the required narrow-band voltmeter. Moreover, phase information can also be obtained by a simple indirect method. At any frequency, one measures not only the magnitudes $|u_x|$ and $|u_y|$ to give

$$|T| = \frac{|u_y|}{|u_x|} \tag{3}$$

but also the magnitude $|u_z|$ of the third phasor, so that by trigonometric solution of the phasor triangle one obtains

$$\angle T = \pm \cos^{-1}\left[\frac{|u_z|^2 - (|u_x|^2 + |u_y|^2)}{2|u_x||u_y|}\right] \tag{4 a}$$

or, equivalently,

$$\angle T = \pm 2\cos^{-1}\sqrt{\left(\frac{|u_z|^2 - (|u_x| - |u_y|)^2}{4|u_x||u_y|}\right)} \tag{4 b}$$

Although the sign given by eqn. (4) is ambiguous, proper choice is usually obvious from the qualitative nature of the magnitude response and known properties of the loop. The above forms apply when $\angle T$ is in the range $0° < \pm\angle T < 180°$; for the range $180° < \pm\angle T < 360°$, the appropriate form is $\angle T = \pm(360° - \theta)$, where θ is the first or second quadrant angle given by eqn. (4).

In the current-injection method, measurement of the third phasor i_z is straightforward, but in the voltage-injection method measurement of v_z directly is inconvenient because of the requirement to float the voltmeter. Instead (in either method) the phasor sum $|u_z| = |u_x + u_y|$ can be read from the addition of the signals u_x and u_y passing through unity (or equal) gain amplifiers, as indicated in Fig. 4 (*a*).

Equation (4) gives accurate results for the loop-gain phase angle in the important frequency range in the neighbourhood of loop-gain crossover, when $|T| \approx 1$. However, it is ill-conditioned when either $|T| \gg 1$ or $|T| \ll 1$, since then either $|u_y| \gg |u_x|$ and $|u_z| \approx |u_y|$, or $|u_x| \gg |u_y|$ and $|u_z| \approx |u_x|$. This condition is immediately obvious in graphical terms from the phasor diagram illustrated in Fig. 4 (*a*), drawn for $|T| > 1$: clearly, small errors in the measurement of the magnitude $|u_y|$ or $|u_z|$ can lead to large errors in $\angle T$.

The ill-conditioning defect in the phase measurement of Fig. 4 (*a*) can easily be overcome† by use of unequal gains for u_x and u_y, as shown in Fig.

† Useful suggestions relating to this technique were made by Dr. Yuan Yu of TRW Systems, Inc., and D. J. Packard of the California Institute of Technology and Hughes Aircraft Co.

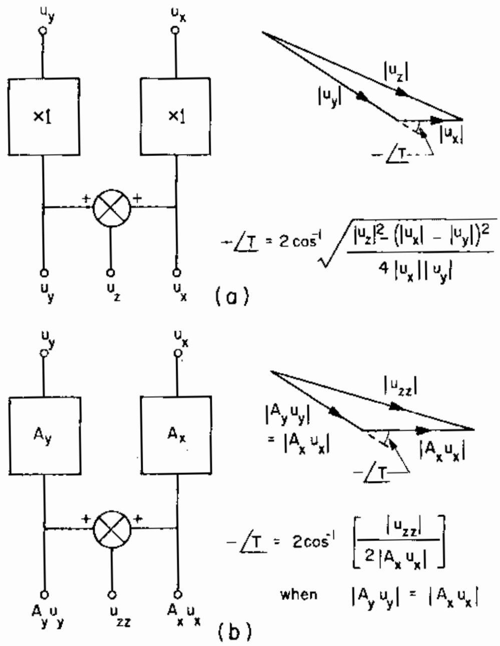

Figure 4. Determination of T, (a) by measurement of the three magnitudes $|u_x|$, $|u_y|$, $|u_z|$; (b) by measurement of the scaled magnitudes $|A_x u_x| = |A_y u_y|$ and $|u_{zz}|$.

4 (b). To the extent that the gains A_x and A_y have zero (or the same) phase, the angle between $A_y u_y$ and $A_x u_x$ determined from the three magnitudes $|A_x u_x|$, $|A_y u_y|$ and $|u_z'| = |A_x u_x + A_y u_y|$ is the same as the angle between u_y and u_x, namely $\angle T$; thus eqn. (4 b), for example, becomes

$$\angle T = \pm 2\cos^{-1}\sqrt{\left(\frac{|u_z'|^2 - (|A_x u_x| - |A_y u_y|)^2}{4|A_x u_x||A_y u_y|}\right)} \tag{5}$$

and can be made well-conditioned at all frequencies by adjustment of the gains A_x and A_y so that all three measured magnitudes are of comparable size. In fact, an additional condition simplifies the procedure considerably: one merely adjusts A_x and A_y so that the magnitudes $|A_x u_x|$ and $|A_y u_y|$ are equal. Let the corresponding magnitude of the summed signal be $|u_{zz}| = |u_z'|$ when $|A_x u_x| = |A_y u_y|$; then eqn. (5) reduces to

$$\angle T = \pm 2\cos^{-1}\left[\frac{|u_{zz}|}{2|A_x u_x|}\right] \tag{6}$$

The practical procedure is therefore to adjust A_x and A_y until equal voltmeter readings $|A_x u_x|$ and $|A_y u_y|$ are obtained, and then to read the corresponding phasor sum $|u_{zz}| = |A_x u_x + A_y u_y|$ for use in eqn. (6). It is not necessary to know either A_x or A_y. As shown in Fig. 4 (b), this procedure scales the two largest phasor magnitudes until they are comparable with the smallest phasor magnitudes, without changing the required loop-gain angle, $\angle T$. The required loop-gain magnitude $|T|$ is of course obtained by setting the two gains equal, $A_x = A_y = A$, and measuring $|Au_x|$ and $|Au_y|$ so that $|T| = |Au_y|/|Au_x| = |u_y|/|u_x|$.

As already mentioned, the original expression for the phase angle $\angle T$, eqn. (4), gives accurate results in the neighbourhood of the loop-gain crossover frequency because $|u_x|$ and $|u_y|$ are already comparable in magnitude without the necessity of scaling by means of the amplifier gains A_x and A_y. In particular, at the crossover frequency, $|u_x| = |u_y|$, so the conditions established by the implementation of Fig. 4 (*b*) exist already without the amplifiers. Therefore, the implementation of Fig. 4 (*a*) may be used directly, and the phase angle at the crossover frequency may be obtained from eqn. (6) with $A_x = 1$ and $u_{zz} = u_z$, or

$$\angle T\big|_{|T|=1} = \pm 2 \cos^{-1}\left[\frac{|u_z|}{2|u_x|}\right] \tag{7}$$

In many applications a measurement of the phase angle solely at the crossover frequency (to determine the phase margin) may be sufficient, so that the amplifier gains A_x and A_y are not needed at all.

To demonstrate the application of the loop-gain-measurement techniques so far discussed, the circuit of Fig. 5 was constructed. The objective was to obtain experimental measurements of the magnitude and phase of the loop gain, without opening the loop. A preliminary expectation is that the loop gain T contains two poles. The point A_v should be suitable for measurement by the voltage-injection method since it satisfies the condition $Z_2 \gg Z_1$, where Z_1, the impedance looking forward round the loop, is greater than 20 k, and Z_2, the impedance looking backwards, is the output impedance of the 709 operational amplifier, which is on the order of 100 Ω.

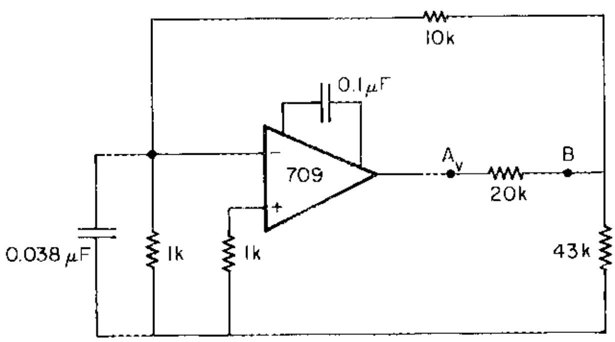

Figure 5. Feedback amplifier circuit for demonstration of loop-gain measurement with voltage injection at point A_v.

The test set-up is shown in Fig. 6. Voltage injection was accomplished through a clip-on current probe ('one-turn secondary'), operated 'backwards' from the oscillator output of a Hewlett–Packard 3590A Wave Analyser. Voltages v_x and v_y were measured with 10 : 1 voltage probes attached respectively to channels 1 and 2 of a Tektronix Type 1A1 Preamplifier in an oscilloscope. The two channels have separately adjustable gains, corresponding to A_x and A_y of Fig. 4 (*b*). Channel 1 polarity is set at 'normal' to read $+A_x v_x$, and channel 2 polarity is set at 'inverted' so that

$-v_y$ is converted to read $+A_y v_y$. The oscilloscope 'vertical out' is connected to the analyser voltage input, and the 1A1 selector switch directs channel 1, channel 2, or the sum of channels 1 and 2, to the voltmeter. Thus, the configuration of Fig. 4 is implemented.

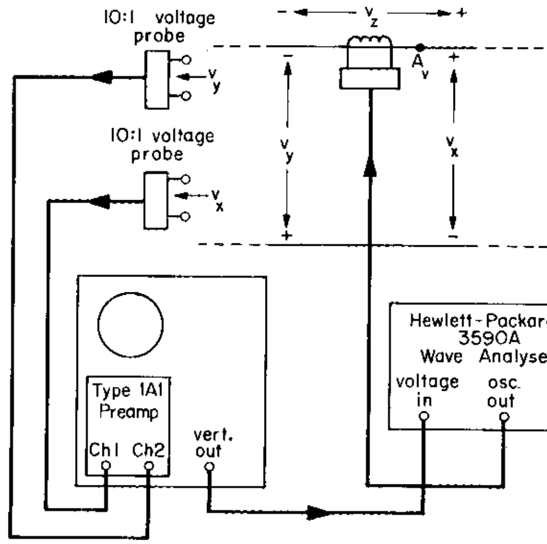

Figure 6. Instrumentation set-up for voltage injection and voltage ratio measurement at point A_v in the circuit of Fig. 5.

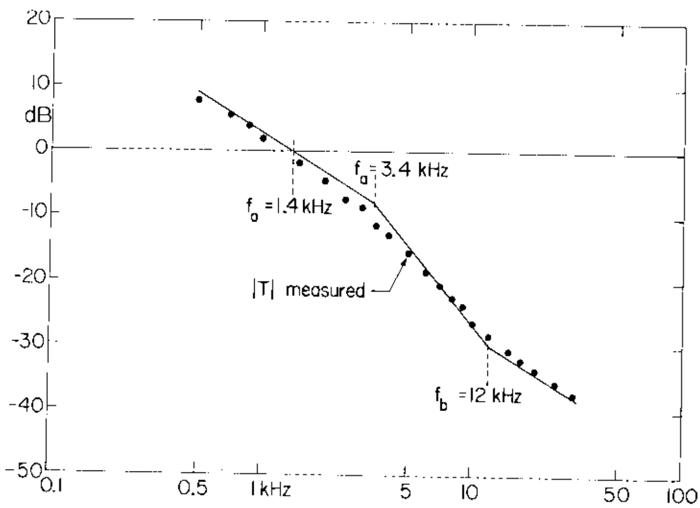

Figure 7. Loop-gain magnitude versus frequency plot obtained by voltage ratio measurements at point A_r in the circuit of Fig. 5.

With the channel 1 and channel 2 gains equal ($A_x = A_y = A$), readings of $|Av_x|$ and $|Av_y|$ were taken, leading to data points for the magnitude $|T|$ of the loop gain as shown in Fig. 7. Best-fit straight-line asymptotes are drawn through the data points, from which it is seen that there is a pole at some low off-scale frequency causing an asymptote zero-dB crossover frequency at $f_0 = 1{\cdot}4$ kHz, another pole at $f_a = 3{\cdot}4$ kHz, and a zero at $f_b = 12$ kHz. The presence of the zero in addition to the two expected poles must be accounted for: presumably, it is due to the gain of the 709 levelling off as the $0{\cdot}1\ \mu$F compensation capacitor becomes essentially a short circuit.

If the loop gain T of the circuit of Fig. 5 were assumed to be a minimum-phase function, the phase response would be implicit in the magnitude response, with a 90° lag from each of the two poles and a 90° lead from the zero, giving a total phase shift at high frequencies asymptotic to $-90°$. Independent measurement of the loop-gain phase angle $\angle T$ by the method described in connection with Fig. 4 (*b*) shows that, on the contrary, the loop gain is not a minimum-phase function. The data points of $\angle T$ obtained by use of eqn. (6) are shown in Fig. 8, and it is seen that $\angle T$ approaches not $-90°$, but $-270°$ at high frequencies. These data are well fitted by asymptotes (45° per decade) that correspond to the two expected left-half plane poles and to a *right*-half plane zero at 12 kHz; consequently, reconsideration of the origin of the zero is required. Examination of the internal circuit of the 709 operational amplifier reveals that the compensation capacitor is in a collector-to-base position, and so the low-frequency phase inversion of the common-emitter amplifier stage is removed when the capacitor becomes an a.c. short-circuit.

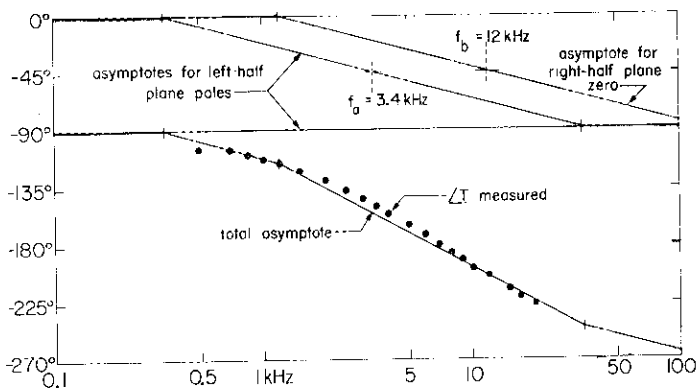

Figure 8. Loop gain phase versus frequency plot obtained for the circuit of Fig. 5.

It is concluded, therefore, that the loop gain T of the circuit of Fig. 5 can be expressed as

$$T = \frac{1 - \dfrac{s}{\omega_b}}{\dfrac{s}{\omega_0}\left(1 + \dfrac{s}{\omega_a}\right)} \tag{8}$$

where

$$f_0 = \omega_0/2\pi = 1{\cdot}4 \text{ kHz} \tag{9}$$

$$f_a = \omega_a/2\pi = 3{\cdot}4 \text{ kHz} \tag{10}$$

$$f_b = \omega_b/2\pi = 12 \text{ kHz} \tag{11}$$

The example has demonstrated the importance of reconciling all features of the measurements with understanding of the physical sources of the effects. The erroneous assumption of a minimum-phase function for T that fitted only the magnitude data points of Fig. 7 would have predicted a greater stability margin than is in fact the case, as follows. Because of the proximity of f_a to f_0, the actual crossover frequency at which $|T|=1$ is 1·3 kHz, slightly less than f_0. The true phase angle at the crossover frequency, from eqn. (8), is

$$\angle T|_{|T|=1} = -[90^\circ + \tan^{-1}(1{\cdot}3/3{\cdot}4) + \tan^{-1}(1{\cdot}3/12)] \tag{12}$$

$$= -[90^\circ + 21^\circ + 6^\circ]$$

$$= -117^\circ \tag{13}$$

giving a phase margin of $180^\circ - 117^\circ = 63^\circ$. If a minimum-phase function had been assumed for T, the phase contribution from the zero at $f_b = 12$ kHz would have been a lead instead of a lag, and the phase angle at the crossover frequency would have been

$$\angle T|_{|T|=1} = -[90^\circ + 21^\circ - 6^\circ]$$

$$= -105^\circ \tag{14}$$

giving a phase margin of $180^\circ - 105^\circ = 75^\circ$, which is 12° greater than the true value of 63°.

3. Measurement of loop gain in unstable loops

In pursuit of the analysis—measurement—correction procedure of system design, it sometimes happens that an actual feedback system unintentionally oscillates, so that the loop-gain measurement cannot be made because the oscillation builds up until limited by non-linearity. One way of restoring the desired design iteration sequence is artificially to reduce the loop gain until oscillation ceases, by introduction of an impedance divider at some convenient point in the loop. The loop-gain measurement is then made, and the true original loop gain deduced by taking account of the correction introduced by the impedance divider. This method is inconvenient, not only because of its indirectness, but also because it may be difficult to account properly for the effect of the impedance divider, since this must be done analytically and its correctness depends upon the system model being correct in the neighbourhood of the impedance divider.

A more satisfactory solution for temporarily extinguishing oscillation is to introduce the impedance divider at the same point where signal injection is made for measurement of loop gain. For the voltage-injection method, an impedance Z_r is introduced in series with the injected voltage, as shown in Fig. 9 (a). The actual loop gain has thereby been reduced by the factor $Z/(Z_r+Z)$, but it is clear that v_y/v_x is still the original, or true, loop gain T. Similarly, for the current-injection method, an impedance Z_i is introduced in parallel with the injected current as shown in Fig. 9 (b), so that the actual loop gain is reduced by the ratio $Z_i/(Z_i+Z)$ but i_y/i_x is still the true loop gain T. Therefore, if the original feedback system oscillates, Z_r can be made large enough, or Z_i small enough, to eliminate the oscillation, yet direct measurement of the gain of the original (unstable) loop can be made and knowledge of the impedance divider ratio is not needed.

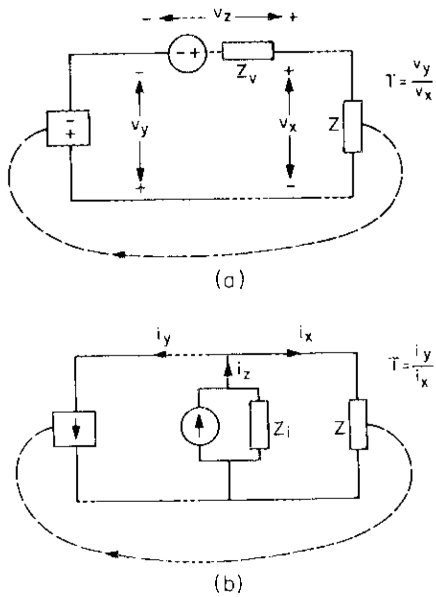

Figure 9. Measurement of T by injection into the closed loop from a non-ideal source, (a) by voltage ratio, (b) by current ratio.

As an example of this technique, a feedback circuit was constructed as shown in Fig. 10. Since the output impedance of the 709 operational amplifier is very low compared to 10 k, point A_v is suitable for measurement of loop gain by the voltage-injection method. The system was purposely made to oscillate, at about 6·7 kHz, by closing switches S_1 and S_2. It was found that insertion of a series resistance greater than 8·2 k at point A_v eliminated the oscillation, thus permitting the loop gain to be measured by voltage injection as in Fig. 9 (a) with Z_v greater than 8·2 k. Data points for the magnitude $|T|$ of the loop gain, with Z_v arbitrarily chosen as 10 k, are shown in Fig. 11.

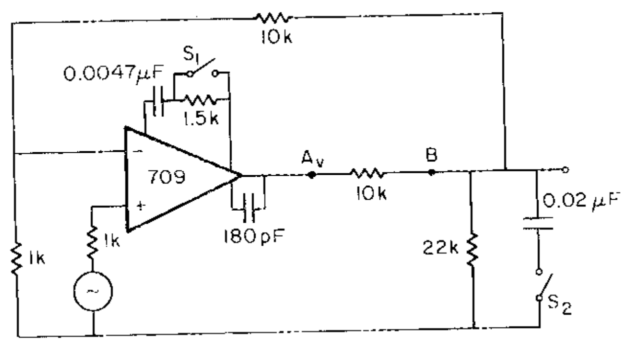

Figure 10. Feedback amplifier circuit for demonstration of unstable loop-gain measurement by voltage injection at A_v (switches S_1 and S_2 closed), and for demonstration of loop-gain measurement by successive voltage and current injection at B (switches open).

Loop-gain crossover occurs at 8·0 kHz, where $|v_x| = |v_y|$, and measurement of the third phasor $|v_z|$ at this frequency gave $|v_z/v_y| = 0{\cdot}11$. The corresponding angle given by eqn. (7) is $\pm 174°$. Since the original system is known to oscillate, the actual phase angle is a lag exceeding 180°, so that the proper solution is $\angle T|_{|T|=1} = -(360° - 174°) = -186°$ (see discussion following eqn. (4)). As a check, the phase angle can be calculated from the measured $|T|$

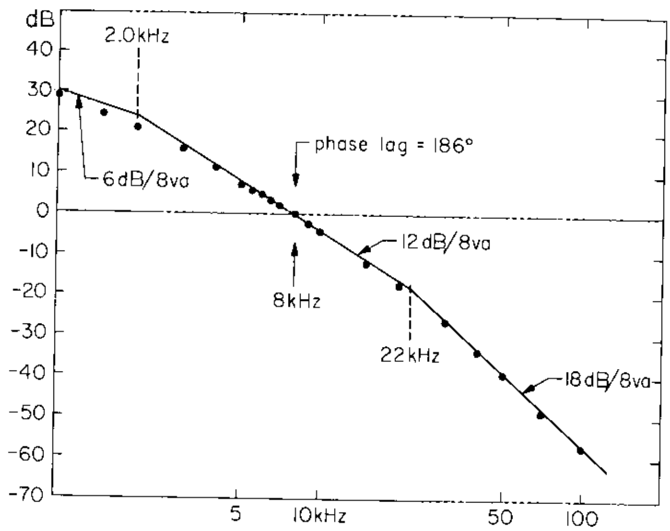

Figure 11. Magnitude versus frequency plot of the unstable loop gain of the circuit of Fig. 10 with switches S_1 and S_2 closed.

versus frequency data of Fig. 11 on the assumption that the loop gain is a minimum-phase function.† There is a pole at some low off-scale frequency, one at 2·0 kHz, and another at 22 kHz ; hence, the phase angle of T at the crossover frequency of 8·0 kHz is given by

$$\angle T|_{|T|=1} = -[90° + \tan^{-1}(8/2) + \tan^{-1}(8/22)]$$

$$= -186° \qquad (15)$$

in excellent agreement with the value directly measured. Hence, the phase margin is $-6°$.

It is therefore demonstrated that loop gain in an unstable system may be directly measured. As a corollary, it may be noted that, even if the original loop is not unstable, the fact that the measured loop gain is independent of Z_r or Z_i indicates that Z_r could be considered part of the source of the injected-voltage signal or Z_i part of the injected current signal, and hence in general the injection can be performed from non-ideal voltage and current sources.

† The circuit under discussion (Fig. 10 with S_1 and S_2 closed) is similar to that of Fig. 5, which was found in § 2 not to have a minimum-phase loop gain. However, the 709 compensation capacitor in Fig. 10 is about 1/20 of that in Fig. 5, so that the corresponding right-half plane zero in T is at about $20 \times 12 = 240$ kHz, above the range for which data points are shown in Fig. 11.

4. Measurement of loop gain at a point of arbitrary impedance by successive voltage and current injection

To measure loop gain by the methods so far described, an injection point in the loop must be found that is driven either by an ideal voltage generator or an ideal current generator. In general, in an actual system, it may not be possible to find an injection point that satisfies either of these extreme conditions. In the switching regulator of Fig. 3, for example, success of the current-injection method at point A_i depends upon the inequality $Z_2 \gg Z_1$; however, since Z_2 represents the output impedance of a transistor, Z_2 certainly declines in magnitude at increasing frequencies owing to the collector capacitance component. In either the voltage or current-injection method, inaccuracy in measurement of T will occur if the appropriate impedance inequality does not hold.

To examine this more general case, consider a point in the feedback loop at which the driving signal is represented neither by an ideal voltage source nor by an ideal current source. Such a driving signal can be represented either by a Thévenin equivalent or by a Norton equivalent; the Norton equivalent is arbitrarily chosen for discussion, as illustrated in Fig. 12. Current injection at point A would give the true loop gain T as

$$T = G_m(Z_1 \| Z_2) \tag{16}$$

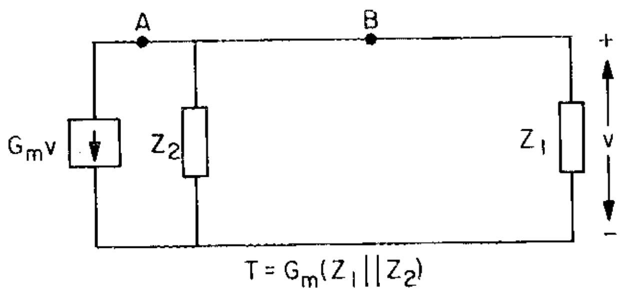

Figure 12. Expression for loop gain T obtained by current injection at A.

Since point A in general is not accessible, let voltage injection from a non-ideal voltage source of impedance Z_r be performed at the accessible point B, representative of a point of arbitrary impedance ratio Z_2/Z_1, as shown in Fig. 13 (a). Measurement of the resulting primed voltages gives a ratio $T_r \equiv v_y'/v_x'$. Analysis of the circuit shows

$$T_r = \left(G_m + \frac{1}{Z_1} \right) Z_2 \tag{17}$$

which is not the same as the true loop gain T. However, elimination of G_m between eqns. (16) and (17) allows the measured ratio T_r to be expressed in terms of the true loop gain T as

$$T_r = \left(1 + \frac{Z_2}{Z_1} \right) T + \frac{Z_2}{Z_1} \tag{18}$$

Next, let current injection from a non-ideal current source of impedance Z_i be performed at the same accessible point B, as shown in Fig. 13 (b).

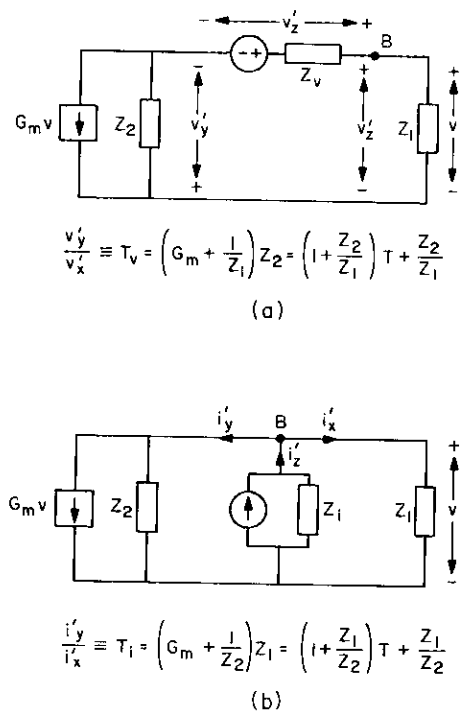

Figure 13. Successive signal injection at the (accessible) point B of arbitrary impedance ratio Z_2/Z_1 in the circuit of Fig. 12, (a) voltage injection and measurement of T_v, (b) current injection and measurement of T_i.

Measurement of the resulting primed currents gives a ratio $T_i \equiv i_y'/i_x'$. Analysis of the circuit shows that

$$T_i = \left(G_m + \frac{1}{Z_2}\right) Z_1 \tag{19}$$

which is not the same as the true loop gain T, but which can be expressed in terms of T as

$$T_i = \left(1 + \frac{Z_1}{Z_2}\right) T + \frac{Z_1}{Z_2} \tag{20}$$

As expected, the inequality $Z_2 \ll Z_1$ leads to $T_v \to T$, so that voltage injection at point B gives the true loop gain, and the opposite inequality $Z_2 \gg Z_1$ leads to $T_i \to T$, so that current injection at point B gives the true loop gain.

In general, for arbitrary Z_1 and Z_2, the true loop gain can be derived from measurement of either T_v or T_i if Z_2/Z_1 is known, but it is clearly more convenient to make both sets of measurements (separately) and then to determine T and, if desired, Z_2/Z_1 from simultaneous solution of eqns. (18) and (20):

$$\frac{1}{1+T} = \frac{1}{1+T_v} + \frac{1}{1+T_i} \tag{21 a}$$

or

$$T = \frac{T_v T_i - 1}{2 + T_v + T_i} \tag{21 b}$$

and

$$\frac{Z_2}{Z_1} = \frac{1 + T_v}{1 + T_i} \tag{22}$$

To illustrate this procedure, voltage and current-injection measurements were separately taken at point B in the circuit of Fig. 10 (switches S_1 and S_2 open). Data points of $|T_v|$ and $|T_i|$ are shown in Fig. 14. Since the T's are phasors, the proper phase relations must be used in evaluation of T from eqn. (21). Although T_v and T_i could be obtained by the phasor triangle measurement described in § 2, in the present case the transfer functions are known to be minimum phase† and so the phases can be inferred from the magnitude responses. This is done implicitly, by inference, from the magnitude plots, of expressions for T_v and T_i in pole-zero form. Thus, in Fig. 14, best-fit

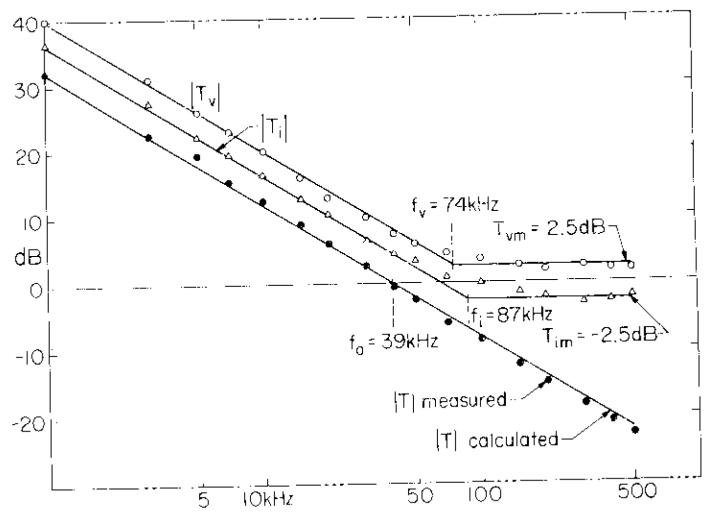

Figure 14. Magnitude versus frequency plots of T_v and T_i measured successively at B in the circuit of Fig. 10 (switches open), the resulting calculated $|T|$, and the data points of $|T|$ measured directly by voltage injection at point A.

straight-line asymptotes are drawn through the data points for $|T_v|$ and $|T_i|$, from which it is seen that

$$T_v = T_{vm}\left(1 + \frac{\omega_v}{s}\right) \tag{23}$$

$$T_i = T_{im}\left(1 + \frac{\omega_i}{s}\right) \tag{24}$$

† The right-half plane zero present in the loop gain of the circuit of Fig. 5 is absent in that of Fig. 10 with S_1 open, because of the presence of the 1·5 k in series with the compensation capacitor.

where

$$T_{vm} = +2{\cdot}5\ \mathrm{dB} \tag{25}$$

$$f_v = \omega_v/2\pi = 74\ \mathrm{kHz} \tag{26}$$

$$T_{im} = -2{\cdot}5\ \mathrm{dB} \tag{27}$$

$$f_i = \omega_i/2\pi = 87\ \mathrm{kHz} \tag{28}$$

Substitution of eqns. (23) and (24) into eqn. (21) leads to

$$T = \frac{\omega_0}{s} \frac{1 + \dfrac{s}{\omega_1} + \left(\dfrac{s}{\omega_2}\right)^2}{1 + \dfrac{s}{\omega_3}} \tag{29}$$

where

$$\frac{1}{\omega_0} = \frac{1}{T_{vm}\omega_v} + \frac{1}{T_{im}\omega_i} \tag{30}$$

$$\frac{1}{\omega_1} = \frac{1}{\omega_i} + \frac{1}{\omega_v} \tag{31}$$

$$\frac{1}{\omega_2^{\,2}} = \frac{T_{vm}T_{im} - 1}{T_{vm}T_{im}\omega_v\omega_i} \tag{32}$$

$$\frac{1}{\omega_3} = \frac{2 + T_{vm} + T_{im}}{T_{vm}\omega_v + T_{im}\omega_i} \tag{33}$$

Insertion of numerical values from eqns. (25) to (28) gives

$$f_0 = \omega_0/2\pi = 30\ \mathrm{kHz} \tag{34}$$

$$f_1 = \omega_1/2\pi = 40\ \mathrm{kHz} \tag{35}$$

$$f_2 = \omega_2/2\pi = \infty \tag{36}$$

$$f_3 = \omega_3/2\pi = 40\ \mathrm{kHz} \tag{37}$$

Hence, since $\omega_1 = \omega_3$ and $\omega_2 = \infty$, the result for T is

$$T = \frac{\omega_0}{s} \tag{38}$$

The magnitude $|T|$ of the true loop gain calculated from the measured $|T_r|$ and $|T_i|$ is thus a straight line of -6 dB/octave slope with crossover at $f_0 =$ 39 kHz, as shown in Fig. 14. Since, as has already been seen, the point A_r in this circuit meets the condition for the voltage-injection method to give directly the true loop gain, data points for $|T|$ were thus obtained and are also shown in Fig. 14. The calculated straight-line asymptote clearly agrees with the measured data points.

For completeness, the ratio Z_2/Z_1 may be determined by substitution of eqns. (23) and (24) into eqn. (22) as

$$\frac{Z_2}{Z_1}=n\frac{1+\dfrac{s}{\omega_4}}{1+\dfrac{s}{\omega_5}} \tag{39}$$

$$n=\frac{T_{rm}\omega_r}{T_{im}\omega_i} \tag{40}$$

$$\omega_4=\frac{T_{rm}}{1+T_{rm}}\,\omega_r \tag{41}$$

$$\omega_5=\frac{T_{im}}{1+T_{im}}\,\omega_i \tag{42}$$

Insertion of numerical values gives

$$n=1\cdot 5 \tag{43}$$

$$f_4=\omega_4/2\pi=42\ \mathrm{kHz} \tag{44}$$

$$f_5=\omega_5/2\pi=37\ \mathrm{kHz} \tag{45}$$

As a check, it can be seen by inspection of the circuit of Fig. 10 that $Z_1=22\|(10+1)=7\cdot 3$ k and $Z_2=10$ k, so that $Z_2/Z_1=10/7\cdot 3=1\cdot 4$. Thus, the predicted expression of eqn. (39) is inaccurate both in low-frequency value and in that Z_2/Z_1 should not be a function of frequency, that is, the zero and pole should cancel.

Review of this method of determination of true loop gain T, from separate measurements of T_r and T_i at an arbitrary injection point, reveals that inaccuracy is an inherent defect. It is seen from eqn. (21 *b*) that if T is very small, the product T_rT_i must approach unity. This can also be seen from eqns. (18) and (20), wherein $T_r\to Z_2/Z_1$ and $T_i\to Z_1/Z_2$ when $T\to 0$. Consequently, it is concluded that beyond the loop-gain crossover frequency, when $|T|$ declines below unity, T_r and T_i each becomes dominated by Z_2/Z_1 and insensitive to T, so that use of eqn. (21) to calculate T from T_r and T_i necessarily gives inaccurate results. This effect is seen in the numerical example based on the circuit of Fig. 10, in which $\omega_2=\infty$ from eqn. (32) because $T_{rm}T_{im}=1$. Indeed, the numerical results of this example gave better accuracy than one has a right to expect, because a small error in the product $T_{rm}T_{im}$ would make ω_2 finite, thereby introducing a spurious zero into the predicted loop gain. Conversely, if the true loop gain were to have additional zeros or poles beyond the crossover frequency, experimental determination of T from T_r and T_i would predict them with very poor accuracy, and might not detect them at all.

An improved method to overcome this accuracy defect is introduced in the next section.

5. Improved measurement of loop gain at a point of arbitrary impedance ratio by null double injection

The problem, restated from the previous section, is to derive the true loop gain of a feedback system by signal injection and measurements at an accessible point that satisfies neither of the extreme inequalities $Z_2 \ll Z_1$ or $Z_2 \gg Z_1$. The problem is represented in Fig. 12, in which the point B is accessible ; the true loop gain is

$$T = G_m(Z_1 \| Z_2) \tag{46}$$

but cannot be directly measured if point A is inaccessible.

It may be shown as follows that the desired result is obtained if two sets of measurements are made, each involving simultaneous voltage and current injection at point B as indicated in Fig. 15. By superposition, each voltage and current indicated in Fig. 15 can be represented by a linear sum of two terms, proportional respectively to the injected voltage and to the injected

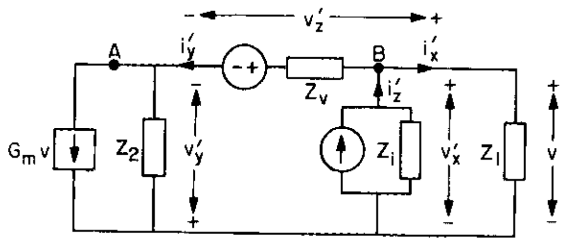

$$\left.\begin{aligned} T_v^n &\equiv \left.\frac{v_y'}{v_x'}\right|_{i_y'=0} = G_m Z_2 \\ T_i^n &\equiv \left.\frac{i_y'}{i_x'}\right|_{v_y'=0} = G_m Z_l \end{aligned}\right\} \Rightarrow \left\{\begin{aligned} &\frac{1}{T_v^n} + \frac{1}{T_i^n} = \frac{1}{G_m(Z_l \| Z_2)} = \frac{1}{T} \\ &\frac{T_v^n}{T_i^n} = \frac{Z_2}{Z_l} \end{aligned}\right.$$

Figure 15. Null double injection of voltage and current at point B in the circuit of Fig. 12, and measurement of the null ratios T_v^n and T_i^n.

current. Each such voltage or current can be nulled to zero by a respectively unique ratio of injected voltage to injected current. If, in particular, the injected voltage and injected current are adjusted with respect to each other so that i_y' is nulled, measurement of the corresponding values of v_x' and v_y' gives a 'null ratio' T_v^n which, by inspection of Fig. 15, is easily seen to be

$$T_v^n \equiv \left.\frac{v_y'}{v_x'}\right|_{i_y'=0} = G_m Z_2 \tag{47}$$

Further, if the injected voltage and injected current are instead adjusted with respect to each other so that v_y' is nulled, measurement of the corresponding values of i_x' and i_y' gives a 'null ratio' T_i^n which is seen to be

$$T_i^n \equiv \left.\frac{i_y'}{i_x'}\right|_{v_y'=0} = G_m Z_1 \tag{48}$$

It follows immediately that

$$\frac{1}{T_v^n}+\frac{1}{T_i^n}=\frac{1}{G_m}\left(\frac{1}{Z_1}+\frac{1}{Z_2}\right) \tag{49}$$

and so, from eqn. (46),

$$\frac{1}{T}=\frac{1}{T_v^n}+\frac{1}{T_i^n} \tag{50 a}$$

or

$$T=\frac{T_v^n T_i^n}{T_v^n+T_i^n} \tag{50 b}$$

and, directly from eqns. (47) and (48),

$$\frac{Z_2}{Z_1}=\frac{T_v^n}{T_i^n} \tag{51}$$

The true loop gain T, therefore, can be determined by eqn. (50) from measurements of the null ratios T_v^n and T_i^n, where each null ratio is established by a specific relation between simultaneously injected voltage and current. It is to be noted that it is not necessary to know what this specific relation is; it is merely necessary to establish the relation by nulling the appropriate voltage or current.

It is seen that eqn. (50) does not suffer from the inherent accuracy defect of eqn. (21), since eqn. (50) does not involve the small difference of two nearly equal numbers. Consequently, use of the null double-injection method and the associated eqn. (50) gives the same accuracy whether T is small or large, and so useful results can be obtained to well beyond the loop-gain crossover frequency. The practical implementation of the null double-injection method is, however, somewhat more complicated than the less accurate successive injection method of the previous section.

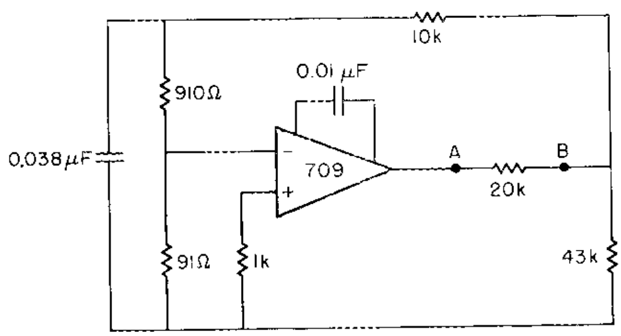

Figure 16. Feedback amplifier circuit for demonstration of loop-gain measurement by the null double-injection method at point B.

To demonstrate the improved method, the circuit of Fig. 16 was constructed and null double injection was performed at point B with the instrumentation illustrated in Fig. 17. Voltage injection was accomplished through a clip-on current probe with a ten-turn secondary, operated 'backwards' from the oscillator output of a Hewlett–Packard 3590A Wave Analyser. Simultaneous

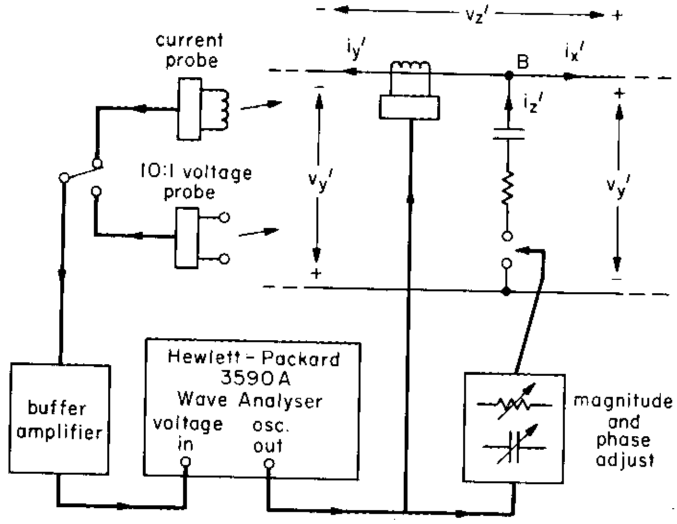

Figure 17. Instrumentation set-up for the null double-injection measurements at point B in the circuit of Fig. 16.

current injection was accomplished through a blocking capacitor and series resistor. Since all quantities of concern are phasors, nulling of a signal requires individual magnitude and phase adjustment of the injected current with respect to a given injected voltage, so the injected current was derived via a phase-shifting network from the same source as the injected voltage. Voltage and current measurements were taken with appropriate probes.

The experimental technique is as follows. To measure $T_v{}^n$, the analyser input is connected to the current probe to read i_y', and i_y' is nulled out by appropriate settings of the magnitude and phase adjustments. Then, the

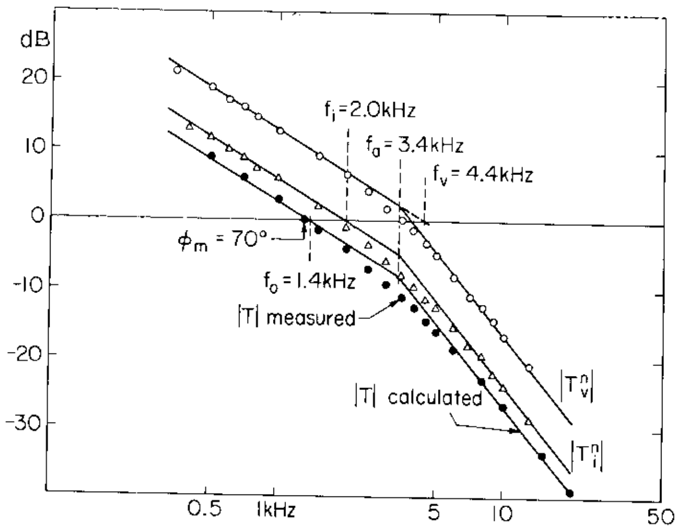

Figure 18. Magnitude versus frequency plots of $T_v{}^n$ and $T_i{}^n$ measured by null double injection at B in the circuit of Fig. 16, the resulting calculated $|T|$, and data points of $|T|$ measured directly at point A.

analyser input is switched to the voltage probe and $|v_y'|$ and $|v_x'|$ are measured. The corresponding ratio is $|T_r^n|$, and the data points are shown in Fig. 18. Similarly, to measure T_i^n, the analyser input is connected to the voltage probe to read v_y', and v_y' is nulled out by appropriate magnitude and phase adjustment. Then, the analyser input is switched to the current probe and $|i_y'|$ and $|i_x'|$ are measured. The corresponding ratio is $|T_i^n|$, and data points are also shown in Fig. 18.

As described in § 2, independent phase information could be obtained by measurement of the third phasor but, again, since the transfer functions in this case are known to be minimum phase,† the pole-zero forms for T_r^n and T_i^n can be deduced from the magnitude plots. Thus, in Fig. 18, best-fit straight-line asymptotes are drawn through the data points for $|T_r^n|$ and $|T_i^n|$, from which it is seen that

$$T_r^n = \frac{1}{\dfrac{s}{\omega_r}\left(1+\dfrac{s}{\omega_a}\right)} \tag{52}$$

$$T_i^n = \frac{1}{\dfrac{s}{\omega_i}\left(1+\dfrac{s}{\omega_a}\right)} \tag{53}$$

where

$$f_a = \omega_a/2\pi = 3{\cdot}4 \text{ kHz} \tag{54}$$

$$f_r = \omega_r/2\pi = 4{\cdot}9 \text{ kHz} \tag{55}$$

$$f_i = \omega_i/2\pi = 2{\cdot}0 \text{ kHz} \tag{56}$$

Substitution of eqns. (52) and (53) into eqn. (50) leads to

$$T = \frac{1}{\dfrac{s}{\omega_0}\left(1+\dfrac{s}{\omega_a}\right)} \tag{57}$$

where

$$\frac{1}{\omega_0} = \frac{1}{\omega_r} + \frac{1}{\omega_i} \tag{58}$$

and insertion of numerical values gives

$$f_0 = \omega_0/2\pi = 1{\cdot}4 \text{ kHz} \tag{59}$$

The magnitude $|T|$ of the true loop gain calculated from the measured $|T_r^n|$ and $|T_i^n|$, obtained from eqn. (57), is also shown in Fig. 18. As a check, since the point A in Fig. 16 is accessible and satisfies the condition for voltage-injection measurements to give directly the true T, such measurements were made and the data points also shown in Fig. 18 clearly verify the calculated $|T|$.

† The circuit of Fig. 16 is similar to that of Fig. 5, and in fact has the same values of f_0 and f_a. However, because the 709 compensation capacitor is only 1/10 that in Fig. 5, the corresponding right-half plane zero in T is at about $10 \times 12 = 120$ kHz, well above the range for which data points are shown in Fig. 18.

Because f_a is close to f_0, the actual crossover frequency is 1·3 kHz, slightly less than f_0. Measurement of the third phasor $|v_z|$ at this frequency gave $|v_z/v_y| = 1{\cdot}15$, and the corresponding angle given by eqn. (7) is $\angle T|_{|T|=1} = -110°$. This agrees with the result obtained from eqn. (57), namely

$$\angle T|_{|T|=1} = -[90° + \tan^{-1}(1{\cdot}3/3{\cdot}4)]$$
$$= -111° \tag{60}$$

The impedance ratio Z_2/Z_1 may be found by substitution of eqns. (52) and (53) into eqn. (51) as

$$\frac{Z_2}{Z_1} = \frac{\omega_r}{\omega_i} = 2{\cdot}2 \tag{61}$$

By inspection of the circuit of Fig. 16, it is seen that $Z_1 \approx 43\|(10+1) = 8{\cdot}8$ k and $Z_2 = 20$ k, so that $Z_2/Z_1 = 20/8{\cdot}8 = 2{\cdot}3$, in good agreement with the experimentally determined value.

It has thus been demonstrated that the null double-injection method permits accurate determination of the true loop gain T at a point where neither $Z_2 \ll Z_1$ nor $Z_2 \gg Z_1$.

The circuit of Fig. 16, chosen for illustration of the null double-injection method, was purposely designed to have a second pole in T beyond the loop-gain crossover frequency in order to verify that accurate results could be obtained for this case even for frequencies well above crossover. The circuit is particularly poorly conditioned for measurement of T by the previous successive voltage and current-injection method. As a matter of interest, the ratios T_r and T_i that would be obtained by separate injection at point B can be determined by substitution of eqns. (57) and (61) into eqns. (18) and (20) as

$$T_r = \frac{Z_2}{Z_1} \frac{1 + \dfrac{1}{Q_r}\left(\dfrac{\omega_p}{s}\right) + \left(\dfrac{\omega_p}{s}\right)^2}{1 + \dfrac{\omega_a}{s}} \tag{62}$$

where

$$\omega_p = \sqrt{(\omega_a \omega_i)} \tag{63}$$

$$Q_r = \sqrt{\frac{\omega_i}{\omega_a}} \tag{64}$$

and

$$T_i = \frac{Z_1}{Z_2} \frac{1 + \dfrac{1}{Q_i}\left(\dfrac{\omega_q}{s}\right) + \left(\dfrac{\omega_q}{s}\right)^2}{1 + \dfrac{\omega_a}{s}} \tag{65}$$

where

$$\omega_q = \sqrt{(\omega_a \omega_r)} \tag{66}$$

$$Q_i = \sqrt{\left(\frac{\omega_r}{\omega_a}\right)} \tag{67}$$

Insertion of numerical values from eqns. (54) to (56) gives

$$f_p = \omega_p/2\pi = 2{\cdot}6\ \mathrm{kHz} \tag{68}$$

$$Q_v = 0{\cdot}77 \tag{69}$$

$$f_q = \omega_q/2\pi = 3{\cdot}9\ \mathrm{kHz} \tag{70}$$

$$Q_i = 1{\cdot}1 \tag{71}$$

The corresponding asymptotes for $|T_v|$ and $|T_i|$ are shown in Fig. 19, along with data points obtained by direct measurement at point B with separate voltage and current injection. Good agreement is obtained, but obviously any attempt to work the problem in the other direction, that is, to deduce T from the measured data points of $|T_v|$ and $|T_i|$, would be futile.

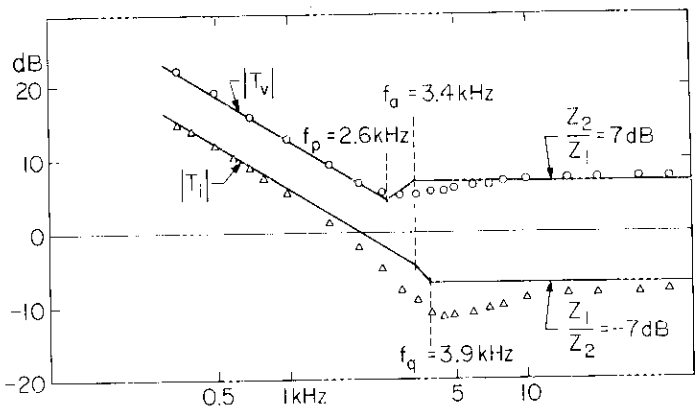

Figure 19. Data points of magnitude versus frequency plots of T_v and T_i measured by successive voltage and current injection at B in the circuit of Fig. 16, and asymptotes calculated from the known loop gain T. Attempts to deduce T from the measured data points would be futile.

Finally, it may be noted that the null double-injection method (and also the successive voltage and current-injection method) at a point B of arbitrary impedance ratio can also be used to measure unstable loop gains. In the derivation based upon the circuit of Fig. 15 (and also Fig. 13), the results are independent of the source impedances Z_v and Z_i respectively of the non-ideal voltage and current-injection sources. Consequently, Z_v can be made large enough, or Z_i small enough, to extinguish any oscillation originally present, in the same way as previously described for injection at a point A where $Z_2 \ll Z_1$ or $Z_2 \gg Z_1$.

6. Reconsideration of loop-gain measurement by voltage or by current injection

Although the null double-injection method described in the previous section permits the loop gain T to be measured at a point of arbitrary impedance ratio Z_2/Z_1, it is obviously much simpler in practice if an injection point can be found at which the impedance ratio is sufficiently small or sufficiently large that either the voltage-injection or current-injection method alone can be used. In this section attention will be focused on conditions for which this simpler procedure is acceptable.

In § 2 the practical example represented by the circuit of Fig. 5 was discussed, and the loop gain was measured by voltage injection at point A_r. It was concluded that the magnitude and phase measurements of T were consistent with the expression for T given in eqn. (8).

If the measurements on the circuit of Fig. 5 are extended an additional decade or so in frequency, it is found that the magnitude response deviates substantially from the -6 dB/octave final asymptotic slope shown in Fig. 7, whereas the phase response does not deviate from the $-270°$ final asymptote shown in Fig. 8. The extended results are shown in Figs. 20 and 21.

The question now arises as to whether the magnitude deviation occurs because the actual loop gain does indeed have such a characteristic, or because the measurement is giving a false result. Further consideration of the circuit gives no cause for modification of the loop gain form given by eqn. (8), so

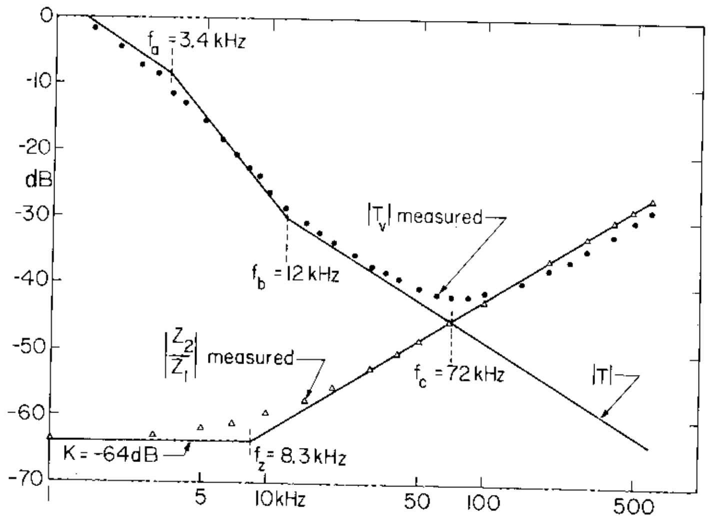

Figure 20. Extended frequency range magnitude versus frequency plot obtained by voltage ratio measurements at point A_r in the circuit of Fig. 5, and $|Z_2/Z_1|$ data obtained by signal injection at point B with the 0·038 μF capacitor short-circuited.

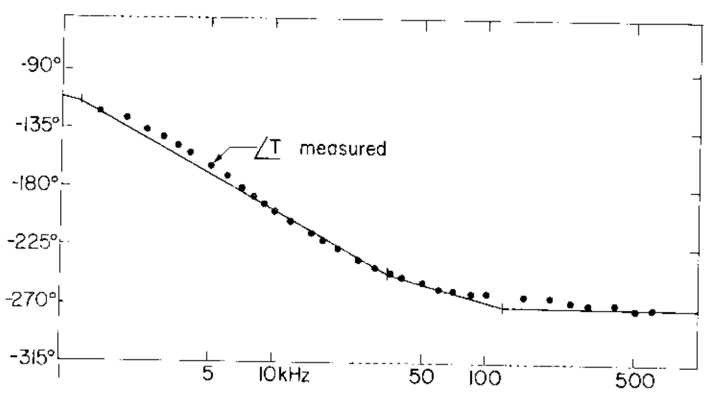

Figure 21. Extended frequency range phase versus frequency plot obtained for the circuit of Fig. 5.

attention is turned to the measurement. What is actually being measured is not T, but T_r; the relation between them is given in eqn. (18):

$$T_r = \left(1+\frac{Z_2}{Z_1}\right) T + \frac{Z_2}{Z_1} \tag{72}$$

The requirement for T_r to be essentially equal to T is not only that $Z_2/Z_1 \ll 1$, but also that $Z_2/Z_1 \ll T$, and this second condition is much more restrictive than the first, beyond loop-gain crossover when $T \ll 1$. To determine whether violation of this second condition is responsible for the magnitude deviation observed in Fig. 20, an independent measurement of Z_2/Z_1 is needed. In principle, the ratio Z_2/Z_1 could be obtained from eqn. (22) as

$$\frac{Z_2}{Z_1} = \frac{1+T_r}{1+T_i} \tag{73}$$

In the frequency range of interest, $T_r \ll 1$, as observed from Fig. 20, and it is expected that $Z_2/Z_1 \ll 1$, so that $T_i \gg 1$. Consequently, eqn. (73) reduces approximately to

$$\frac{Z_2}{Z_1} = \frac{1}{T_i} \tag{74}$$

and so a measurement of T_i by current injection at point A_r in the circuit would give the required ratio Z_2/Z_1. In practice, however, this measurement was not possible because of dynamic range limitations: the ratio Z_2/Z_1 is so small (at low frequencies) that an injected signal capable of giving a readable i_r (even with the narrow-band voltmeter of a wave analyser) required an i_y that overloaded the output of the 709. Therefore, recourse was taken to a different method in which the output impedance Z_2 of the 709 was measured independently by application of a test voltage v_1 (through a blocking capacitor) to point B in the circuit of Fig. 5, with the 0·038 μF capacitor short-circuited to disable the feedback, and measurement of the resulting voltage v_2 at point A_r. The impedance Z_2 was then determined from

$$|Z_2| \approx \frac{|v_2|}{|v_1|} \times 20 \text{ k} \tag{75}$$

The impedance Z_1 may be calculated directly from the circuit as $Z_1 = 20 + (43 \| 10) = 28$ k (in the frequency range of interest, above f_a). The resulting measurements of $|Z_2/Z_1|$ are also shown in Fig. 20, and the best-fit straight-line asymptotes indicate that

$$\frac{Z_2}{Z_1} = K\left(1+\frac{s}{\omega_z}\right) \tag{76}$$

where

$$K = 6{\cdot}3 \times 10^{-4} \rightarrow -64 \text{ dB} \tag{77}$$

$$f_z = \omega_z/2\pi = 8{\cdot}3 \text{ kHz} \tag{78}$$

It is clear from Fig. 20 that the measured $|T_r|$ changes from following $|T|$ to following $|Z_2/Z_1|$, within acceptable experimental error, when $|Z_2/Z_1|$ exceeds $|T|$, so that T_r is given by eqn. (72) with $Z_2/Z_1 \ll 1$:

$$T_r = T + \frac{Z_2}{Z_1} \tag{79}$$

The analytic expression for T_r, obtained by substitution of eqns. (8) and (76) into eqn. (79), is

$$T_r = \frac{\left(1 - \dfrac{s}{\omega_b}\right)\left(1 - \dfrac{s}{\omega_c}\right)\left(1 + \dfrac{s}{\omega_c}\right)}{\dfrac{s}{\omega_0}\left(1 + \dfrac{s}{\omega_a}\right)} \tag{80}$$

where

$$\omega_c = \sqrt{\left(\frac{\omega_0 \omega_a \omega_z}{K \omega_b}\right)} \tag{81}$$

Substitution of the previously determined numbers gives $f_c = 72$ kHz, in satisfactory agreement with the intersection of the $|T|$ and $|Z_2/Z_1|$ asymptotes in Fig. 20.

Since the right- and left-half plane zeroes in eqn. (80) give zero net contribution to the phase angle, $\angle T_r$ given by eqn. (80) is the same as $\angle T$ given by eqn. (8), in agreement with the measurements of Fig. 21.

It may be concluded, therefore, that the actual loop gain T of the circuit of Fig. 5 is indeed given by eqn. (8), and that the deviation from T observed in the measured T_v at higher frequencies occurs because of the breakdown of the condition $Z_2/Z_1 \ll T$, in spite of the validity of the condition $Z_2/Z_1 \ll 1$. The actual loop gain $|T|$ does in fact continue to decrease at -6 dB/octave, and does not increase as do the $|T_v|$ measurements. This example illustrates the importance of understanding whether the magnitude measurements taken by signal injection are or are not equal to the actual loop-gain magnitude at frequencies beyond crossover, when $|T| \ll 1$.

7. Conclusions

Practical methods of measuring loop gain T in feedback systems, including switching-mode regulators, have been discussed. Methods of measurement by voltage injection and by current injection into a closed-loop system are reviewed : if a point in the loop can be found at which the impedance Z_2 looking backward is sufficiently smaller than the impedance Z_1 looking forward, voltage injection is appropriate ; conversely, if a point can be found at which Z_2 is sufficiently greater than Z_1, current injection is appropriate. Measurement of both magnitude and phase of T is discussed, and it is shown how the phase can be determined indirectly by measurement of three phasor magnitudes. Possible ill-conditioning of the formula for phase can be eliminated by appropriate scaling of the three measured magnitudes.

A first extension of the method of measurement of loop gain without opening the loop is concerned with loop-gain measurement when the system is unstable. By lowering the loop gain at the point of signal injection, the oscillation can be inhibited and yet a direct measurement of the unstable loop gain can still be made. This permits the system to be properly characterized so that appropriate corrective measures may be taken.

A second extension is concerned with loop-gain measurement when points at which Z_2 is sufficiently smaller or sufficiently greater than Z_1 are inaccessible. It is shown that in principle the true loop gain T can be determined indirectly from measurements T_v and T_i resulting separately from voltage injection and from current injection at an arbitrary point in the loop at which the ratio Z_2/Z_1 may have any value. However, it is found that this method gives inaccurate results above the loop-gain crossover frequency when $|T| < 1$.

A third extension is concerned with an improved method of determination of T by signal injection at a point of arbitrary impedance ratio Z_2/Z_1. In the improved method, the null double-injection method, the true loop gain T is determined from measurements $T_v{}^n$ and $T_i{}^n$, each resulting from simultaneous injection of voltage and current with specific adjusted magnitude and phase relations. The ratio $T_v{}^n$ is measured with the magnitude and phase adjusted to null the current looking backward from the injection point, and the ratio $T_i{}^n$ is measured with the magnitude and phase relation adjusted to null the voltage looking backward from the injection point. It is shown that this improved method avoids the inaccuracy inherent in the successive voltage-injection and current-injection methods.

Finally, attention is redirected to the measurement of loop gain by the simple voltage or current-injection method, and the conditions to be satisfied by the impedance ratio Z_2/Z_1 at the signal-injection point are reconsidered.

References

1965, *Electron. Design*, **13,** 43.
Spohn, 1963, *Hewlett-Packard J.*, **14,** 5.
1965. *Hewlett-Packard Application Note*, No. 59, 15 January.